BIOCHEMISTRY
including biophysical chemistry & molecular biology

Article

pubs.acs.org/biochemistry

The Conformation of a Catalytic Loop Is Central to GTPase Activity on the Ribosome

Johan Åqvist* and Shina C. L. Kamerlin

Department of Cell & Molecular Biology, Uppsala University, Biomedical Center, Box 596, SE-751 24 Uppsala, Sweden

Supporting Information

ABSTRACT: The translational GTPases hydrolyze GTP on the ribosome at several stages of the protein synthesis cycle. Because of the strong conservation of their catalytic center, these enzymes are expected to operate through a universal hydrolysis mechanism, in which a critical histidine residue together with the sarcin−ricin loop of the large ribosomal subunit is necessary for GTPase activation. Here we examine different possible pathways for GTP hydrolysis by EF-Tu through extensive computer simulations. We show that a conformational change of the peptide plane preceding this histidine has a decisive effect on the energetics of the reaction. This transition was predicted earlier by us and has recently been confirmed experimentally. It is found to promote early proton transfer from water to the γ-phosphate group of GTP, followed by nucleophilic attack by hydroxide ion. The calculated reaction energetics is in good agreement with available kinetic data, for both wild-type and mutant versions of EF-Tu, and indicates that the latter may enforce a change in mechanism toward more concerted pathways.

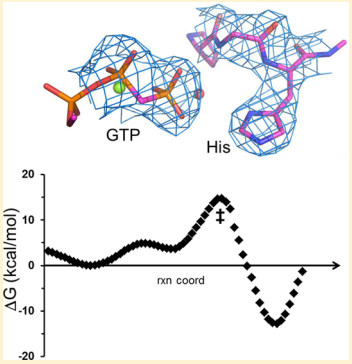

Protein synthesis on the ribosome requires the hydrolysis of GTP at several stages of the translation cycle, such as initiation, peptide elongation, ribosome translocation, termination, and ribosome recycling.[1,2] These GTP hydrolysis reactions are catalyzed by the translational GTPases (trGTPases), which are auxiliary protein factors that are needed for efficient protein synthesis. For example, in bacteria elongation factor Tu (EF-Tu) delivers aminoacyl-tRNAs (aa-tRNA) to the ribosome in a ternary complex with GTP, and the subsequent hydrolysis reaction is triggered upon correct mRNA−tRNA codon−anticodon matching. This then causes the aa-tRNA to donate its amino acid to the growing peptide chain. To effect translocation of the ribosome along the mRNA, elongation factor G (EF-G) also binds to the ribosome in its GTP-bound state. This association event likewise causes the hydrolysis reaction to occur, which in turn moves the last tRNA along with the mRNA from the hybrid A/P state to the P/P state, thereby vacating an empty ribosomal A site with a new codon being presented. The translational GTPases are expected to operate through a universal GTP hydrolysis mechanism due to the strong conservation of their catalytic center, where particularly the histidine residue of the universally conserved PGH motif is the key to GTPase activation.[3,4] The histidine side chain changes its conformation upon binding of the trGTPases to the ribosome, because of its interaction with the critical sarcin−ricin loop (SRL) of the large (50S) ribosomal subunit. This leads it to fall into place for coordinating a water molecule that subsequently attacks the γ-phosphate of GTP (Figure 1).[4−7] There thus appears to be a common mode of binding of the G-domain of all trGTPases to the ribosome, and the active GTPase conformation is achieved only after interaction with the SRL has been established.[4−7]

The mechanism of GTP hydrolysis on the ribosome has been subject to some debate, in particular with regard to the possible role of the histidine as a general base in the reaction.[8,9] Rodnina and co-workers[3] showed that the histidine residue, His84, in EF-Tu (*Escherichia coli* EF-Tu numbering will be used throughout this paper) is critical for catalysis, and that its substitution by alanine reduced the hydrolysis rate by a factor of $>10^6$. The first crystal structure of a trGTPase bound to the ribosome in its activated conformation (obtained with the nonhydrolyzable GTP analogue GDPCP) showed His84 coordinating a water molecule in a seemingly favorable orientation for nucleophilic attack on the γ-phosphate[4] (Figure 1a). This led Voorhees et al. to the natural suggestion that the imidazole side chain would activate the hydrolytic water by abstraction of one of its protons.[4] As demonstrated by Liljas et al.,[8] the situation is more complicated than it initially appears, because the coordination geometry of the water molecule clearly indicates that one of its protons is engaged in a hydrogen bond with the carbonyl group of Thr61. It is also evident that one proton resides between the water molecule and the nearest oxygen of the γ-phosphate, as this distance is very short. This is further reinforced by three recent crystal structures of EF-G bound to the ribosome in its active conformation,[5−7] all of which show the water−γ-phosphate oxygen distance to be significantly shorter than that between the water and the His84 ND1 atom. Hence, if there also is a proton bridging His84 ND1 and the water molecule, the histidine is likely to be doubly protonated, because its NE1 atom must be protonated, because of the interaction with the anionic SRL phosphate (Figure 1a).

Received: November 5, 2014
Revised: December 15, 2014
Published: December 17, 2014

DOI: 10.1021/bi501373g
Biochemistry 2015, 54, 546−556

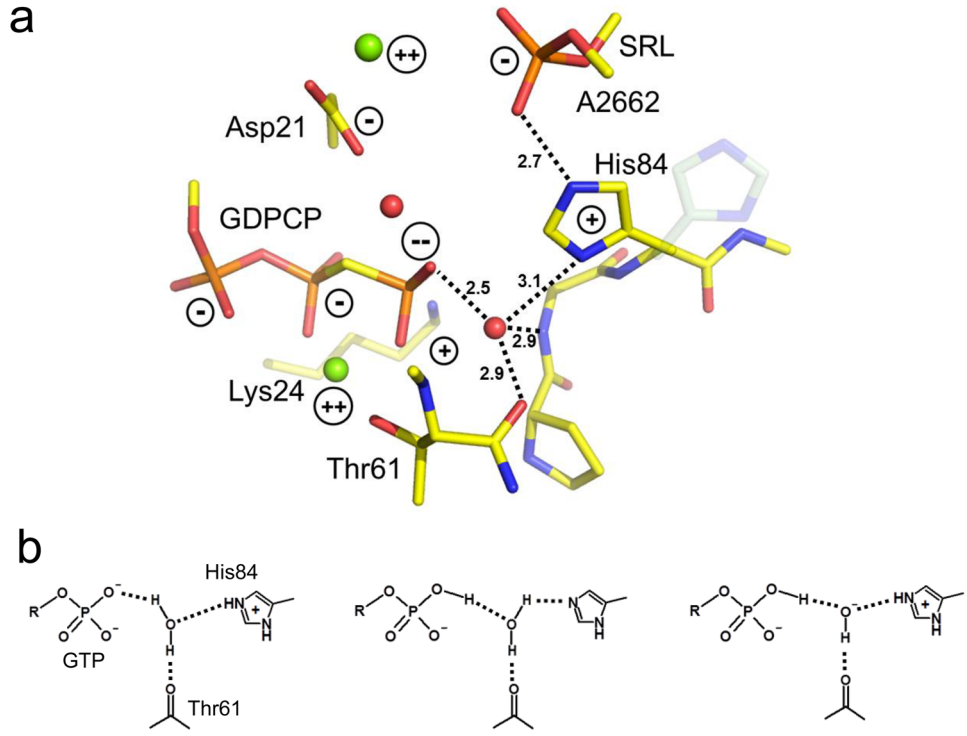

Figure 1. Structure of the reaction center of activated trGTPases on the ribosome. (a) Key residues of the active site from one of the recent complexes with a GTP analogue are shown.[5] His84 is in its activated conformation, and the corresponding inactive conformation is overlaid with transparent cyan carbons. Mg^{2+} ions and water molecules are shown as green and red spheres, respectively, and key H-bond distances are indicated. (b) Different possible protonation states of the nucleophile, γ-phosphate, and His84 that are compatible with the crystal structures.

The situation described above thus casts some doubt on the His84 general base mechanism, and indeed, earlier free energy calculations by us showed that (ground state) proton transfer from the catalytic water to His84 is strongly disfavored because of electrostatic repulsion between the resulting hydroxide ion and the γ-phosphate.[10] Another problem with the His84 general base mechanism is that the reaction shows no pH dependence in the pH range (6−8.5) in which a histidine side chain is expected to normally ionize, with either GTP or its analogue GTP-γ-S as the substrate.[3,11] Taken together, these results strongly suggest that the catalytic reaction does not involve proton transfer with His84. Instead, the structural, biochemical, and computational results indicate that the histidine is positively charged once it has reached the active conformation. In fact, both our calculations and those of others[10,12] predicted that the histidine pK_a is upshifted to >9 because of the presence of several proximal negative charges (Figure 1a), which would explain the insensitivity to pHs below this value. The earlier calculations by us[10] and Adamczyk and Warshel[12] predicted that the reaction may plausibly involve direct attack by water on the γ-phosphate dianion via a substrate-assisted mechanism (transfer of proton to phosphate) and is facilitated by either direct[10] or indirect ("allosteric") electrostatic interactions[12] caused by the charged His84.

A somewhat different mechanism was proposed by Aleksandrov and Field, based on quantum mechanics/molecular mechanics (QM/MM) calculations,[13] where the rate-limiting step instead involves attack of water on the protonated γ-phosphate (monoanion) with the neutral form of His84 acting as a general base. This scenario is not incompatible with the observed pH independence because His84 was assumed to be protonated in the reactant state. However, instead of having an intermediate hydroxide ion state, resulting from the transfer of a proton from water to phosphate, a proton was predicted to be shuttled from and to His84 in the different reaction steps (Figure S1, scheme vii, of the Supporting Information).[13] To further complicate the mechanistic picture, recently determined crystal structures of the GTP-bound forms of the free eukaryotic and archaeal EF-Tu homologues eIF5B and aEF1A clearly show that a monovalent cation is bound between the β- and γ-phosphates.[14] It was argued that this ion cannot be observed with the GTP analogue GDPCD or GDPNP that had been used to obtain crystallographic complexes with the ribosome, as these analogues disrupt the ion coordination. Hence, if such a monovalent cation is indeed present also in the activated state on the ribosome, it could potentially affect the energetics of the catalytic reaction.

To try to reliably resolve the detailed energetics of catalysis by the trGTPases on the ribosome and compare various plausible competing pathways, we have performed a large number of independent computer simulations of possible reaction mechanisms for GTP hydrolysis by activated EF-Tu bound to the bacterial ribosome. These simulations involved both regular free energy calculations between different well-defined states as reported previously[10] and simulations of different reaction mechanisms, utilizing the empirical valence bond (EVB) approach.[15,16] We have further examined the effect of different EF-Tu mutations, different protonation states of His84, and the presence of the monovalent cation discussed above.

MATERIALS AND METHODS

MD Simulations. All MD simulations were performed as reported previously[10,17] with the MD package Q,[18] utilizing the OPLS-AA force field (Macromodel 9.1, Schrödinger LCC, New York, NY).[19] Spherical simulation systems (40 Å in diameter) centered on the γ-phosphorus atom of GTP were used after solvation by a TIP3P water droplet of the same size. All protein

DOI: 10.1021/bi501373g
Biochemistry 2015, 54, 546−556

and RNA atoms outside the simulation sphere were tightly restrained to their initial coordinates with a force constant of 200 kcal mol^{-1} Å^{-2} and excluded from nonbonded interactions. A restraint of 10 kcal mol^{-1} Å^{-2} to the initial coordinates was applied to solute atoms within the outermost 2 Å shell of the spherical systems. Water molecules close to the sphere boundary were subjected to radial and polarization restraints according to the SCAAS model.[18,20] Initial coordinates were taken from our previously reported equilibrated simulation system.[10] These were based on the crystal structure of the ribosome-bound EF-Tu ternary complex[4] [Protein Data Bank (PDB) entries 2XQD and 2XQE] that contains no ions or water molecules (with the exception of the catalytic water and GTP-bound Mg^{2+} ion), complemented by interior solvent molecule positions from two high-resolution structures of free EF-Tu ternary complexes (PDB entries 2C78 and 1EXM).[21,22] Also, a structurally important K^+ ion ligated by Asp50 and Glu55, identified earlier in these structures,[10] was included in our simulations. Mg^{2+} counterions placed at electrostatic potential minima were added to the system, and charged groups <5 Å from the simulation boundary were neutralized as described previously[23] to prevent insufficiently screened charges from exerting an unphysical influence on the system. RNA backbone phosphate charges in this region were also neutralized by counterion smearing. As noted earlier[10] and discussed further below, this simulation system predicted stable Mg^{2+} ion positions that were found to coincide well with crystallographically observed electron density peaks.[4,5] Importantly, it also showed convergence of the backbone conformation of the critical PGH motif to that observed in the high-resolution structures of free EF-Tu ternary complexes[21,22] and also subsequently seen in recent structures of activated EF-G (Figure 2).[5,6]

The MD simulations were conducted using a 1 fs time step, in combination with the SHAKE procedure[24] for solvent bonds and angles. A 10 Å cutoff was employed for direct nonbonded interactions, with electrostatic interactions beyond the cutoff treated by the local reaction field multipole expansion method.[25] No cutoff was applied to nonbonded interactions involving the central part of the system that is treated by the EVB model (i.e., the triphosphate moiety of GTP, the hydrolytic water molecule, and the side chain of His84). A large number of MD simulations were conducted for different reaction mechanisms and EF-Tu mutants (see Results), where the free energy perturbation (FEP) umbrella sampling method was used to drive the system between the different EVB states.[15,16] Each such simulation consisted of an equilibration phase with stepwise heating from 1 to 300 K with the gradual release of restraints on heavy solute atoms, followed by 800 ps of unrestrained equilibration at 300 K. Each system was then subjected to 1.1−2.2 ns of production phase MD for calculations of free energy profiles, which comprised 21 intermediate FEP windows. Four to eight replicate simulations were performed for each system with randomized initial velocities reassigned during equilibration according to the Maxwell distribution.

EVB Models. The different possible reaction mechanisms considered here were described by the EVB method[15,16] and are shown in Figure 3 and Figure S1 of the Supporting Information, where the valence bond states involved in each case are indicated. Calibration of the EVB reaction surfaces followed the standard procedure[16,26] and involved running MD/FEP simulations for each of the mechanisms in a water sphere (also 40 Å in diameter), using the same protocol that is described above for the ribosome simulations. From these calculations, the EVB specific calibration parameters (i.e., off-diagonal Hamiltonian matrix elements and gas phase energy shifts between EVB states)[16,26] were determined by fitting the resulting free energy profiles to available information for the solution reactions. The relevant EVB parameters used in this work, as well as atomic charges for the nonstandard phosphate moieties, are provided in Figures S1 and S2 of the Supporting Information.

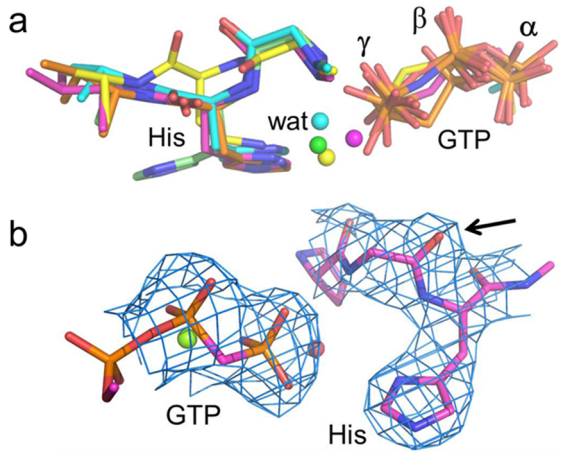

Figure 2. (a) Comparison of different active site conformations of the trGTPases showing the earlier EF-Tu ternary complex with the ribosome[4] (yellow carbons), the recently determined complexes[5,6] with EF-G (magenta[5] and orange[6] carbons), the predicted MD structure (cyan carbons) of the activated EF-Tu complex,[10] and a high-resolution structure of the (inactive) free ternary complex of EF-Tu (green carbons).[21] The catalytic water molecule (if observed) is colored accordingly. (b) Calculated $2F_o - F_c$ electron density from experimental structure factors[5] around the catalytic histidine residue, where the carbonyl group of the preceding glycine is marked with an arrow (the calculated density for ref 6 shows a similar characteristic carbonyl bump).

The reaction free energy for the transfer of a proton from the nucleophilic water molecule to the γ-phosphate is obtained from the relationship $\Delta G^0_{PT}(aq) = 2.303RT[pK_a(donor) - pK_a(acceptor)]$, which yields a ΔG^0_{PT} of 12.2 kcal/mol based on pK_a values of 6.7 and 15.7 for GTP and water, respectively. The corresponding activation barrier can be accurately estimated from experimental linear free energy relationships between proton transfer rates and donor−acceptor pK_a differences,[27,28] which in our case yields an activation barrier ($\Delta G^{\ddagger}$) of 15.7 kcal/mol. For calibration of the barrier for the attack of OH^- on the γ-phosphate monoanion (Figure 4a,b), the most relevant experimental data pertain to the corresponding attack on phosphate di- and triesters with aryl leaving groups.[29,30] Here, two important effects influence the reaction rate. The first is neutralization of the phosphate charge, as seen by comparing the di- and triester rates, and this corresponds to a decrease in the activation barrier of ~4.6 kcal/mol.[29,31] This is relevant to our case because the strongly bound Mg^{2+} ion effectively neutralizes the single β- and γ-phosphate negative charges of protonated GTP. The second effect is due to protonation of one of the γ-phosphate oxygens, which allows the resulting hydroxyl group to interact favorably (via hydrogen bonding) with the incoming nucleophile and/or departing leaving group. Via comparison of the experimental hydrolysis rates for methyl-2,4-dinitrophenyl phosphate and the (protonated) monoanion of 2,4-dinitrophenyl phosphate,[29] this effect can be seen to reduce the activation barrier by as much as 2 kcal/mol, even for a neutral water nucleophile. Earlier quantum mechanical calculations including solvation effects yielded an even larger effect of H-bonding and predicted the barrier for attack of OH^- on neutral methylphosphate to be as low as 13 kcal/mol at (approximately) a 1 M standard state.[32] While this

DOI: 10.1021/bi501373g
Biochemistry 2015, 54, 546−556

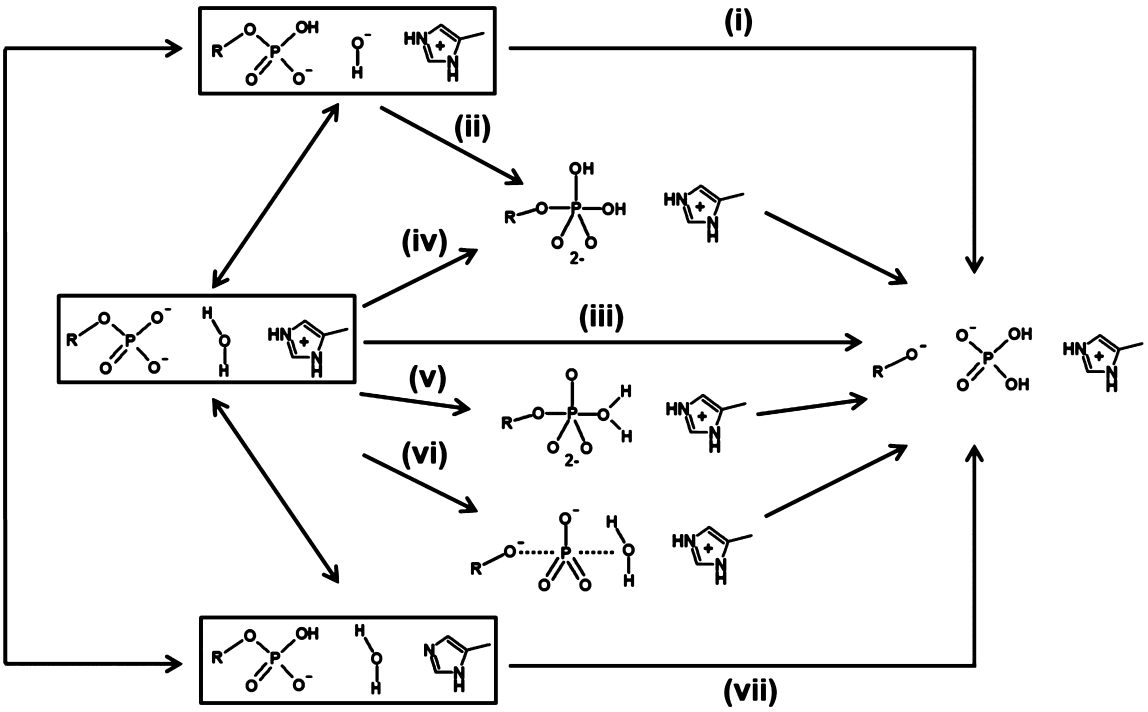

Figure 3. Schematic representation of the different reaction pathways considered in the EVB simulations. The three possible protonation states of the nucleophile, γ-phosphate, and His84, compatible with the crystal structures, are boxed.

could be an underestimation, it likely provides a lower bound for the free energy barrier. An upper bound is provided by the experimental rate of attack of OH^- on the methyl-2,4-dinitrophenyl phosphate monoanion, lacking both the charge neutralization and H-bonding effects, for which the barrier is 22.2 kcal/mol at a 1 M standard state.[29] Hence, considering both of the effects mentioned above, the rates of attack of OH^- on the triesters provide a reasonable estimate for our reference reaction. These have been given for both aryl esters of cyclic and noncyclic dialkyl phosphates,[29,30] and the corresponding free energy barriers are 17−18 kcal/mol at a 1 M standard state of the nucleophile. We will thus use a value here of 17.5 kcal/mol, which is also the average of the lower and upper bounds discussed above, and this then yields an overall barrier of 12.2 + 17.5 = 29.7 kcal/mol for the hydroxide mechanism and a corresponding predicted rate of 2×10^{-9} M^{-1} s^{-1} at 300 K.

The neutral water mechanisms considered here involve both concerted and stepwise GTP hydrolysis pathways, as well as associative and dissociative variants (Figure 4c−f and Figure S1 of the Supporting Information). These mechanisms were all calibrated to an overall barrier of 27 kcal/mol at a 55 M standard state of water according to the linear free energy relationship reported in ref 33. This is also the same reference value used by Adamcyk and Warshel in their calculations.[12] The similarity in barrier heights for these different neutral water mechanisms is further supported by quantum mechanical calculations on the hydrolysis of Mg^{2+}-monomethyl pyrophosphate, with a leaving group pK_a (6.5) similar to that of GDP.[34] For putative mechanisms with transient high-energy intermediate states, these were generally modeled as symmetrical processes with the intermediate just a few kilocalories per mole below the flanking barriers. For the stepwise associative mechanism with late proton transfer to phosphate considered in ref 12 (Figure 4d), we used the same calibration as reported therein, again with an overall barrier of 27 kcal/mol at the 55 M standard state. Finally, the activation free energy barrier of the general base mechanism (Figure 4g), in which neutral His84 assists the attack of water on the γ-phosphate monoanion, was estimated to be reduced by 3 kcal/mol, yielding a $\Delta G^{\ddagger}$ of 24 kcal/mol, in accordance with the observed effect of protonation on the hydrolysis of *p*-nitrophenyl phosphate[33] as well as pyrophosphate.[35]

The calibration strategy described above for the uncatalyzed solution reaction mechanisms is thus aimed at using consensus values for the overall activation free energy barriers, which are all close to the value of 27 kcal/mol derived from experimental measurements.[12,33] The exceptions are the hydroxide and general base mechanisms, which have slightly higher and lower barriers, respectively. Hence, while there is naturally some uncertainty with regard to the detailed energetic differences between different uncatalyzed reaction pathways, it turns out that the effects of the ribosome EF-Tu environment on the different pathways are very clear-cut, and therefore, their feasibility can be unambiguously judged from the MD/EVB simulations.

Electron Density Calculations. To more closely examine the experimental support for the backbone conformation of the PGH motif observed in recent ribosome-bound EF-G structures (Figure 2),[5,6] electron density maps were calculated using standard procedures. The split PDB coordinate files (4JUW and 4JUX,[5] and 4BTC and 4BTD[6]) and the structure factor data were downloaded from the PDB. For each structure, the coordinate files were hand edited to produce one large coordinate file, and a structure factor calculation was conducted using a bulk solvent correction and isotropic scaling[36] with the Phenix system.[37] The σ_A-weighted $(2m|F_o| - D|F_c|)$ electron density maps[38] were calculated within Phenix.

RESULTS

Analysis of New Relevant Crystal Structures. Since the publication of the first crystal structure of activated EF-Tu bound to the 70S bacterial ribosome in 2010,[4] several recent structures

DOI: 10.1021/bi501373g
Biochemistry 2015, 54, 546−556

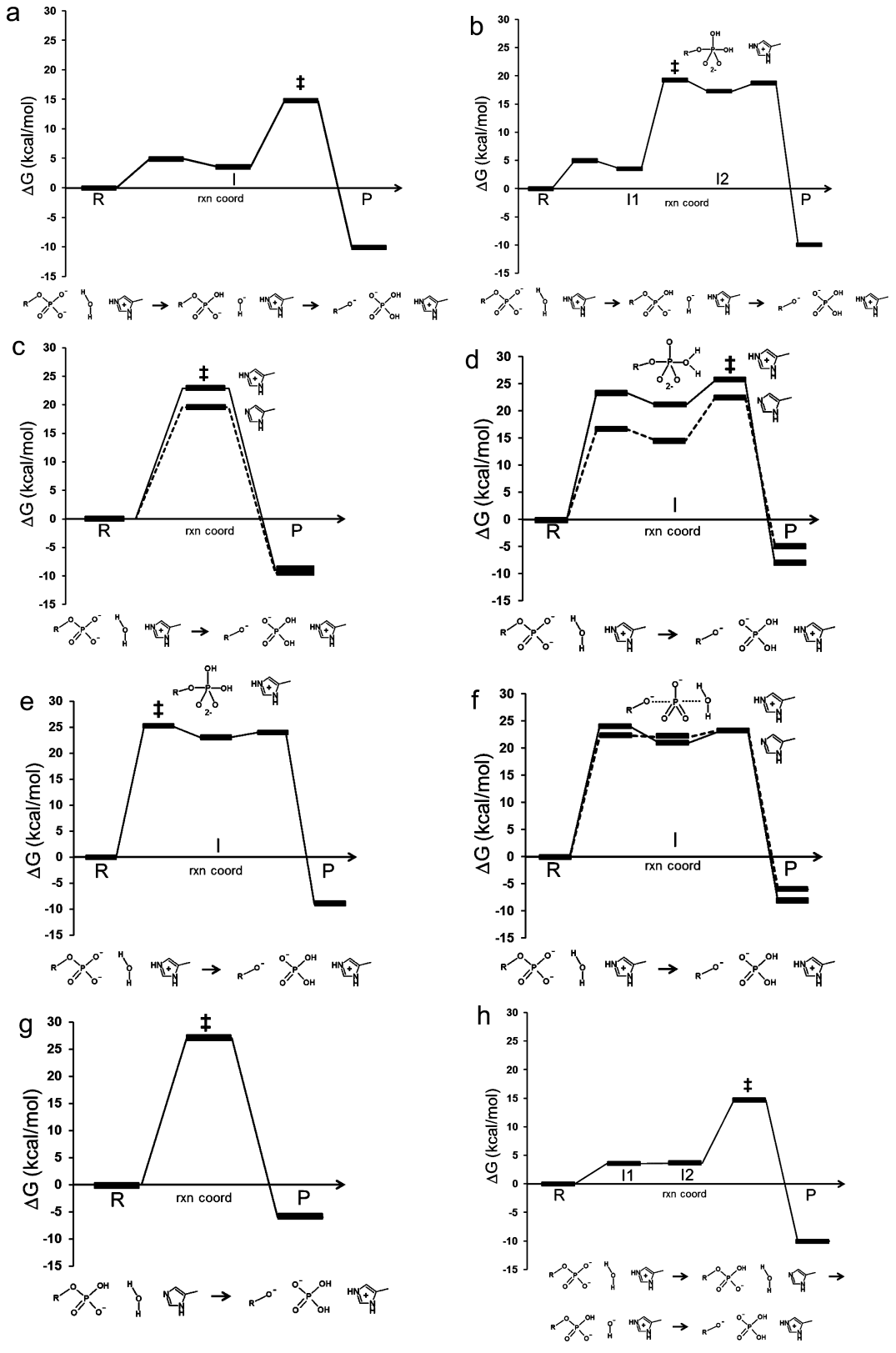

Figure 4. Summary of calculated free energy profiles for the different reaction pathways examined (see the text). The reaction paths in panels a–f are different variants of the net reaction in which a water molecule attacks the γ-phosphate dianion of GTP. Panel g denotes the concerted general base-assisted attack of water on the monoanion (protonated) γ-phosphate with a neutral His84 and panel h the corresponding stepwise path starting from same reactant state as in panels a–f.

of activated complexes with EF-G have also been reported.[5−7] Two of these new structures now have a few extra Mg^{2+} ions included in the crystallographic model, and it is noteworthy that the two Mg^{2+} ions predicted earlier by us[10] have been confirmed experimentally.[5,6] One of these is in a region (between Asp21 and the A2662 phosphate) where it contributes to neutralization of

DOI: 10.1021/bi501373g
Biochemistry 2015, 54, 546−556

negative charge near the reactants. In fact, counting the charges in the active site region of the complex shows that the electrostatics is perfectly balanced (i.e., a neutral active site) with His84 being protonated (Figure 1a). Considering the short distances between the catalytic water molecule and the γ-phosphate, His84, and the carbonyl group of Thr61 in all available structures,[4−7] the logical conclusion is that each of these three interactions with the water oxygen is bridged by a proton. There are thus basically three possible charge states that best explain the crystal structures (Figure 1b): (1) a γ-phosphate dianion, neutral water, and protonated His84, (2) a γ-phosphate monoanion, neutral water, and neutral His84, and (3) a γ-phosphate monoanion, hydroxide ion, and protonated His84. The energetics of these different possible charge states is, of course, considerably important for the actual chemical reaction mechanism as will be discussed below.

However, there is also another feature of the new crystal structures of activated EF-G complexes that appears to be of major importance. Two of these structures[5,6] now show the backbone of the invariant PGH motif in a conformation significantly different from that determined previously,[4] with the peptide plane preceding the histidine residue flipped by ∼90° (Figure 2a). This new backbone conformation is essentially identical to that found in high-resolution structures of free ternary complexes with nonhydrolyzable GTP analogues.[21,22] Also, as reported earlier by us,[10] MD simulations repeatedly converged to this structure (Figure 2a), which with the protonated histidine side chain strongly stabilizes negative charge at the center of this "anion hole"-like structural motif. Such stabilization pertains both to a possible hydroxide ion, resulting from the transfer of a proton to the γ-phosphate, and to the inorganic phosphate product.[10] Hence, while this peptide flip is not discussed in either of the structural reports[5,6] and may seem to be a minor detail of these large structures, we would argue that it could be of considerable importance for the actual mechanism of GTP hydrolysis. That is, as a result of this flip, a large additional dipole of ∼4 D is now positioned with its positive end directly interacting with the catalytic water molecule. Thus, computer simulations based on the "old" conformation would be expected to yield different energetics if they do not capture this apparently crucial conformational change, as is verified below. The fact that our earlier MD simulations[10] did predict the transition thus lends further support to their validity in our opinion.

The new conformation of the translational GTPase active site thus makes sense from a catalytic point of view and because it agrees with that observed in structures of free ternary complexes. It actually renders structural rearrangements within the G-domain minimal upon activation and basically restricts these to the histidine side chain. Furthermore, the conformation is now clearly supported by the electron density maps (Figure 2b) and also has a more usual peptide plane orientation as indicated by the pep-flip measure,[39] which is reduced from 2.71 to 1.83 Å. The φ and ψ angles of the histidine residue now have normal values of −68.5° and 150.5°, respectively, while in the earlier EF-Tu structure[4] (as well as in the EF-G structure of ref 7), they are in a disallowed region (41.1° and −166.5°, respectively).

Energetics of Different Possible Reaction Mechanisms. We have used the empirical valence bond (EVB) method[15,16] to evaluate the energetics of different reaction schemes, with configurational sampling by molecular dynamics (MD) simulations. These reaction schemes are summarized in Figure 3 and Figure S1 of the Supporting Information. Free energy profiles (potentials of mean force) along the reaction paths were obtained with the free energy perturbation (FEP) umbrella sampling approach, as described extensively elsewhere.[16,26] In addition to these reaction path simulations, we also assessed the EVB results for some of the key intermediate charge states with regular FEP calculations as reported previously.[10] There are three main classes of mechanisms for the GTP hydrolysis reaction that have to be considered. These are (1) those that involve early proton transfer (PT) to the γ-phosphate, resulting in subsequent nucleophilic attack on the γ-phosphate monoanion by hydroxide (Figure 3, paths i and ii), (2) mechanisms that involve neutral water attack and later PT to the γ-phosphate dianion, which can be either concerted or stepwise (paths iii−vi), and (3) general base mechanisms involving PT to neutral His84, which again can have either concerted (path vii) or stepwise character. Note also that there is clearly no room in the crystal structures[5,6] for mechanisms involving two water molecules, where one may assist the other by general base catalysis and eventual PT to the phosphate.

Early PT Mechanisms. Our earlier free energy calculations of the activated EF-Tu complex on the ribosome showed that the hydroxide ion state is significantly stabilized because of strong hydrogen bonding with the conserved PGH motif and the favorable electrostatic interaction with the positively charged His84.[10] This stabilization also completely vanished when His84 was either deprotonated or moved to its inactive conformation. We have further the refined the energetics of the putative hydroxide ion state by additional longer MD/FEP simulations and by considering protonation of each of the possible phosphate oxygens for the γ-phosphate monoanion, both in the ribosome complex and in solution. It is clear that protonation of the O3 phosphate oxygen is most favorable, and the current best estimate for the free energy stabilization of the hydroxide state, relative to the corresponding PT from water to phosphate in solution,[10] is $\Delta\Delta G_{PT} = -8.3 \pm 0.6$ kcal/mol. With an estimated free energy cost (ΔG_{PT}^{wat}) from pK_a values of 12.2 kcal/mol for the solution process, this yields a predicted free energy of the hydroxide ion state that is <4 kcal/mol above the presumed resting state with the dianion, neutral water, and protonated His84.

EVB simulations of the actual proton transfer reaction from water to phosphate yield a similarly strong stabilization of the hydroxide ion state (Figures 4a and 5), with a free energy profile that does not involve a high barrier and where the product state of the PT step is only 3.6 kcal/mol above the reactant state. Hence, PT from water to the γ-phosphate is facile and the hydroxide ion state strongly stabilized, as evidenced by two different types of calculations. As discussed further below, this effect originates mainly from favorable interactions with the PGH motif, where the correct conformation of its backbone is clearly important. As reported earlier, MD simulations of the hydroxide ion state spontaneously convert to the correct backbone conformation even if they are initiated from the flipped backbone structure.[10] We also quantified the effect of the incorrect backbone conformation of the PGH motif by restraining it to the corresponding original structure,[4] and the result is a $\Delta\Delta G_{PT}$ of -2.6 ± 0.5 kcal/mol. That is, the hydroxide ion state is destabilized by almost 6 kcal/mol because of the wrong backbone conformation.

Starting from the intermediate hydroxide ion state resulting from PT to the γ-phosphate, we examined both concerted (path i) and stepwise (path ii) phosphoryl transfer between the leaving group and nucleophile. It can be seen from the free energy profiles in panels a and b of Figure 4 that the transition state for

DOI: 10.1021/bi501373g
Biochemistry 2015, 54, 546−556

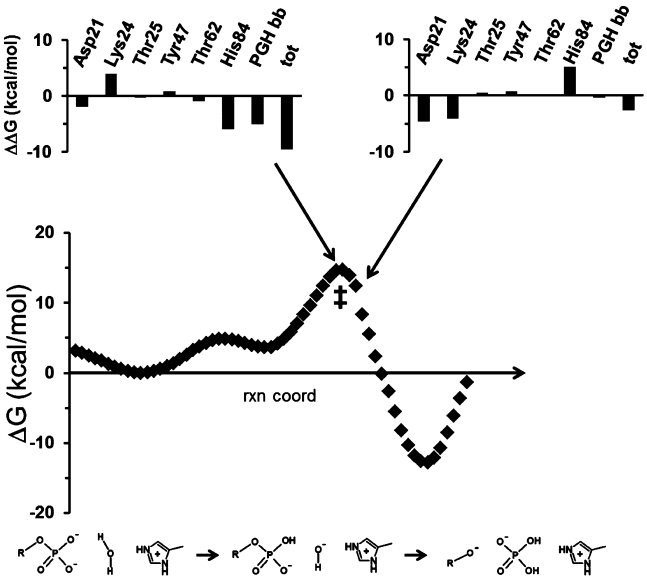

Figure 5. Detailed free energy profile for the favored hydroxide mechanism. Free energy contributions of key active site groups are given in the top panels at the transition state and just after it, relative to the reactant state. These group contributions refer to amino acid side chains, except for "PGH bb", which denotes interactions with the backbone of the PGH motif. The group contributions were obtained by converting the corresponding average interaction energies to free energies by the linear response approximation as in ref 12.

the concerted mechanism is predicted to be ~2 kcal/mol lower than for the stepwise process that involves a transient high-energy pentavalent phosphorane intermediate. The free energy barrier for concerted hydroxide attack is predicted to be 11.1 kcal/mol, which with the above estimate of 3.6 kcal/mol for the initial PT step yields an overall reaction barrier of 14.7 kcal/mol. It can be noted that this prediction is in good agreement with the available experimental data,[3,11] and the overall catalytic effect corresponds to a barrier reduction of ~15 kcal/mol compared to that of the uncatalyzed reaction. A representative MD snapshot of the transition state ensemble for this mechanism is shown in Figure 6a.

Neutral Water Attack Mechanisms. We further examined a number of different types of mechanisms that involve water (rather than hydroxide) attack on the γ-phosphate dianion (paths iii–vi), and the corresponding free energy profiles are summarized in Figure 4c–f. The most favorable of these reaction pathways (iii) turns out to be the concerted water attack reported by Adamczyk and Warshel (their calculations gave a barrier of ~18 kcal/mol for both the concerted and stepwise paths).[12] However, our calculations yield a more favorable barrier for this concerted mechanism when His84 is uncharged, in which case the activation free energy is 19.6 kcal/mol (Figure 4c). The corresponding barrier is predicted to be 23 kcal/mol with the doubly protonated histidine. Although it is not entirely clear what the His84 protonation state is in ref 12 (Figure 5 and Figure S2 of ref 12 depict it as singly protonated), their barrier of 18 kcal/mol is in reasonable agreement with the results obtained herein. However, it seems clear from our simulations that this mechanism cannot compete with the hydroxide ion pathway discussed above. The stepwise associative mechanism with late PT to phosphate,[12] involving a pentacoordinated intermediate in which the nucleophile retains both its protons (path v), was also considered here. These calculations were again conducted with

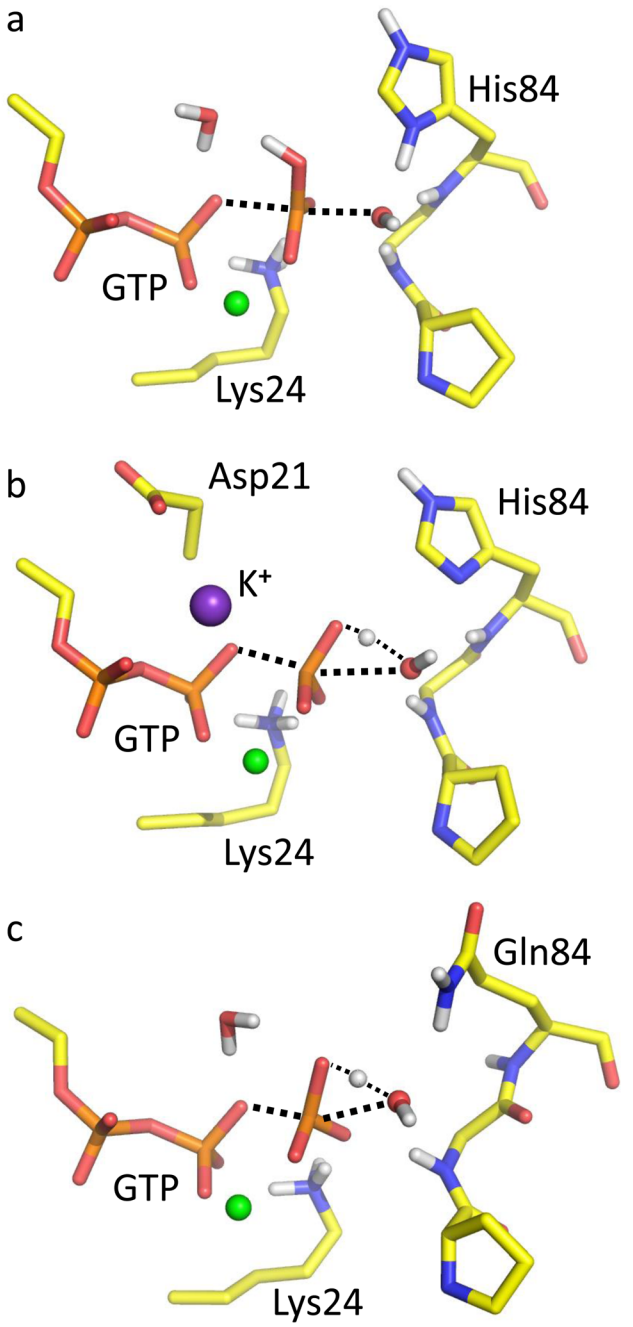

Figure 6. Representative MD snapshots from the transition state ensembles of the favored mechanisms of the native reaction (a), the reaction with a K^+ ion between Asp21 and the substrate triphosphate (b), and the reaction with the H84Q mutant of EF-Tu (c).

both protonation states of His84, and the corresponding reaction free energy profiles give activation barriers of 25.7 and 22.5 kcal/mol with the charged and uncharged histidine, respectively (Figure 4d). That is, again we find that this type of mechanism is more favorable with the neutral His84, but the barrier is too high compared to experiment.[3,11]

We further examined mechanisms with stepwise attack of neutral water on the γ-phosphate for the two limiting cases (paths iv and vi) in which either a pentavalent phosphorane intermediate with complete PT from the nucleophile (Figure 4e) or a dissociative metaphosphate-like intermediate is transiently formed (Figure 4f). For the former associative pathway, which

DOI: 10.1021/bi501373g
Biochemistry 2015, 54, 546–556

has a −2 charge on the phosphorane intermediate, the predicted free energy barrier is 25 kcal/mol (with protonated His84) and thus somewhat higher than that of the fully concerted variant. The dissociative pathway has axial P−O bond lengths of 2.4−2.5 Å in the TS and little charge development on the nucleophile, but considerable charge transfer to the leaving group. Here, the obtained activation free energy is 23 kcal/mol with neutral His84 and 1 kcal/mol higher when the histidine is charged (Figure 4f). These results can be summarized in such a way that, because the neutral water attack mechanism transition states do not involve any significant charge movement to the right in Figure 1 (i.e., toward His84), the otherwise advantageous effect of the protonated histidine (see above) basically goes away. In particular, transition states that mainly involve separation of one negative charge between the β- and γ-phosphates are not stabilized very much in the ribosomal complex. Hence, the neutral form of His84 works just as well as the protonated form for these types of mechanisms, and the favored path then tends to become concerted because there is no distinct stabilization of high-energy intermediates.

General Base Mechanisms. The general base mechanism proposed originally by Voorhees et al.,[4] in which neutral His84 assists attack of water on the γ-phosphate dianion, seems to ruled out by the fact that all calculations predict a significantly increased pK_a of His84 in the ribosome complex.[10,12,13] Furthermore, our earlier work showed a huge destabilization of proton transfer from water to neutral His84 in the presence of the γ-phosphate dianion.[10] This would mean that the resting state on the ribosome has the histidine doubly protonated, which is natural in view of the presence of several negative charges in its immediate vicinity. Our earlier calculations[10] predicted a pK_a of 9, while Adamczyk and Warshel obtained a value of 11.[12] The prediction from Aleksandrov and Field of a pK_a of 17, with the force field used also in their reaction calculations,[13] seems more unrealistic but clearly indicates a shift in the same direction. However, the latter authors suggested another type of general base mechanism in which a proton is first relayed from the biprotonated His84 via the catalytic water molecule to the γ-phosphate, effectively resulting in a state with neutral His84 and a γ-phosphate monanion. The subsequent attack of water on the protonated phosphate would then be assisted by general base catalysis resulting in proton transfer back to His84 (Figure 3 and Figure S1 of the Supporting Information, path vii). It should, however, be pointed out here that the energetics obtained in ref 13 generally appears to be somewhat uncertain. Not only is a His84 pK_a shift of >10 units unrealistic, but their activation barrier obtained for water attack on the γ-phosphate dianion of ∼45 kcal/mol must also be way off, as it by far exceeds the corresponding barrier for uncatalyzed GTP hydrolysis. As discussed by Warshel and co-workers,[40] using only QM/MM potential energy calculations along selected reaction paths, without configurational sampling or actual free energy calculations, may be a likely explanation for the energetics obtained in ref 13.

Nevertheless, it is interesting to examine the energetics associated with a general base-assisted mechanism for attack of water on the protonated phosphate group, because this appears as a distinct possibility in view of the fact that the normal (unshifted) pK_a values of GTP and histidine are more or less equal. That is, one would expect that the state with neutral His84 and protonated γ-phosphate may have an energy similar to that of the resting state discussed above. In ref 13, PT from His84 to the γ-phosphate was predicted to be ∼5 kcal/mol uphill and the overall barrier for the proposed mechanism was predicted to be 25.1 kcal/mol, which is not particularly close to the experimental free energy barrier of 14 kcal/mol for the hydrolysis reaction on the ribosome.[3,11] We first used regular FEP calculations as described in ref 10 to evaluate the energetics of the state with protonated GTP^{3-} and neutral His84 compared to the resting state with GTP^{4-} and biprotonated histidine. These calculations yielded a ΔG_{PT} value of 3.5 ± 0.4 kcal/mol for PT from His84 to the γ-phosphate on the ribosome using pK_a values of 6.7 and 6.5 for GTP and histidine, respectively, for the corresponding reference simulation in water. This value is, in fact, well in line with our earlier prediction that the His84 pK_a is increased to ∼9.[10] It also shows that the three possible charge states discussed above in the context of the crystal structures are all rather similar in energy with the OH^-/GTP^{3-} and $His84^\circ/GTP^{3-}$ states both being only 3−4 kcal/mol above the $His84^+/GTP^{4-}$ resting state.

The MD/EVB calculations for the subsequent general base-catalyzed step (path vii), in which neutral water attacks the γ-phosphate monoanion and His84 abstracts one of the water protons, yield a free energy barrier of 27 kcal/mol for the concerted variant of this mechanism (Figure 4g). It should be noted here that the general base step is actually predicted here to be anticatalytic because the estimate for the corresponding uncatalyzed barrier is 24 kcal/mol compared to 27 kcal/mol for attack on the γ-phosphate dianion.[12,33] Because the overall barrier for the concerted general base mechanism also includes the free energy cost of PT from His84 to the γ-phosphate (3.5 kcal/mol), the resulting barrier is predicted to be >30 kcal/mol. There is thus no indication from our simulations that this mechanism could be operational on the ribosome. However, it should be noted that the stepwise version of this mechanism, in which neutral His84 abstracts the water proton prior to the nucleophilic attack on the protonated γ-phosphate, becomes equivalent to the hydroxide mechanism (Figure 4h).

Predicted Effects of EF-Tu Mutations and Monovalent Ions. It was recently suggested that a monovalent cation (presumably K^+) coordinated between the α- and γ-phosphate groups could provide a catalytic function in the translational GTPases similar to that of the "arginine finger" in the Ras-RasGAP system.[14] This proposal was based on crystal structures of complexes of GTP with eIF5B and aEF1A, which are eukaryotic and archaeal orthologs of IF2 and EF-Tu, respectively. These structures clearly show a monovalent cation bound between the phosphate groups and also coordinated by the conserved aspartate corresponding to Asp21 in EF-Tu. It was suggested that such a monovalent cation would also play an essential catalytic role on the ribosome and that the reason it had not been discovered earlier is that GTP analogues, such as GDPNP and GDPCP, do not allow the proper coordination to be formed.[14] It should be noted, however, that these crystal structures do not represent ribosome-bound complexes and His84 is flipped out into its inactive conformation.

We therefore conducted a number of simulations, including a K^+ ion initially placed at the observed position, and the results from these calculations can be summarized as follows. First, as soon as His84 is positively charged and placed in its active conformation, this ion is apparently easily exchanged for a water molecule and is observed to move during MD simulations, typically to a position where it interacts with only the α-phosphate and is not strongly bound. Accordingly, the MD/EVB calculations show essentially no effect of the ion on any of the mechanisms described above that have His84 positively charged. The main reason for why the K^+ ion position becomes

DOI: 10.1021/bi501373g
Biochemistry 2015, 54, 546−556

less stable in the ribosome complex is the presence of both the biprotonated His84 in its active conformation and the Mg^{2+} ion observed between Asp21 and the phosphate group of A2662 of the SRL,[5,6] which neutralize the overall charge in the active site (see above). Second, if His84 is uncharged, the K^+ position observed in the free GTP-bound factors[14] is stable also on the ribosome, but it is not predicted to provide any additional catalytic effect.

For the most favorable pathway with neutral His84, namely the concerted water attack discussed above (path iii), the activation free energy actually increases from 20 to 22 kcal/mol with the ion present. This slightly anticatalytic effect becomes more pronounced for the stepwise dissociative path, which reflects the fact that the K^+ ion remains coordinated to the α- and β-phosphates, thereby partly sacrificing its interaction with the γ-phosphate in the transition state (Figure 6b). Thus, the greater the separation between the β- and γ-phosphates in the transition state, the more difficult it is for the ion to bridge all the way between the α- and γ-phosphate groups. This is actually rather different from the arginine finger in RasGAP, which can more easily bridge between the α- and γ-phosphates.[41] Hence, we can conclude that while a GTP-bound monovalent ion may have an effect on the intrinsic GTPase activity of EF-Tu, there appears to be no catalytic advantage of this ion on the ribosome. These results also agree with recent data from Rodnina and co-workers, who found no dependence on monovalent ion concentration of the GTP hydrolysis rate on the ribosome.[11]

Among the EF-Tu mutations recently analyzed experimentally in detail by Rodnina and co-workers,[3,11] two are particularly interesting as they retain significant but considerably reduced GTPase activity despite major side chain substitutions. These are, first, the H84Q mutation, which replaces the presumably positively charged His84 side chain with a neutral polar residue, and, second, the D21A mutation, which removes a negative charge near the β- and γ-phosphate groups (Figure 1a). For the H84Q case, our earlier calculations showed that the glutamine residue strongly destabilizes a mechanism involving a hydroxide ion, as was also found to be case with the H84A mutation.[10] However, the results from these MD/EVB simulations show that the H84Q mutant can indeed provide significant stabilization of a fully concerted TS in which there is less negative charge development on the water nucleophile (path iii). Hence, the predicted activation barrier of H84Q for this concerted mechanism is 20 kcal/mol (Table 1). It can be noted that this free energy barrier is very similar to that obtained for the concerted mechanism with the native His84 side chain in its neutral form. It thus appears that the H84Q mutant retains some activity because it is able to change the mechanism toward a concerted one (Figure 6c) that does not involve strong negative charge development on the nucleophile. The quantitative effect of this mutation of 5.2 kcal/mol on the overall barrier compared to that of the hydroxide mechanism is also in good agreement with the value of 5 kcal/mol estimated by Rodnina and co-workers.[11]

Table 1. Predicted Activation Free Energy Barriers (kilocalories per mole) for EF-Tu Mutations

	favored mechanism	$\Delta G^{\ddagger}$	$\Delta\Delta G^{\ddagger}$
wild type	PT and hydroxide attack	14.7	–
neutral His84	concerted water attack	19.6	4.9
H84Q	concerted water attack	19.9	5.2
D21A	PT and hydroxide attack	19.0	4.3
D21A with neutral His84	concerted water attack	20.0	5.3

The residue corresponding to Asp21 in EF-Tu is strictly conserved in the bacterial trGTPases, while the equivalent position in Ras is a glycine; the arginine finger of RasGAP is instead located close to the Asp21 position in EF-Tu.[41] Together with the fact that His84 corresponds to a glutamine in Ras, this situation indicates that there are fundamental differences between the two types of GTPases that likely also pertain to mechanistic aspects. In fact, from an electrostatic point of view, the presence of the negatively charged Asp21 as well as the positively charged His84 would clearly seem to facilitate movement of negative charge from left to right in Figure 1. If so, the D21A mutation should logically destabilize PT from the catalytic water molecule to the γ-phosphate. This is precisely what the present simulations show, and the cost of forming the hydroxide ion with D21A is predicted to increase to from 4 to 9 kcal/mol. Hence, the main effect of the mutation is to destabilize the proton transfer reaction, while the subsequent nucleophilic attack (path i), in contrast, is found to be much less affected with a calculated free energy barrier of 10 kcal/mol. The overall effect of D21A on the hydroxide mechanism is thus predicted to be ~5 kcal/mol (Table 1), which is in good agreement with the experimental results.[11] However, there is also the possibility that removal of the Asp21 negative charge ~6 Å from His84 may lower the pK_a of the histidine so that it becomes singly protonated. To examine this possibility, we also conducted simulations of the D21A mutant with a neutral His84 and the corresponding favored concerted hydrolysis mechanism (path iii). Interestingly, these calculations show that there is no effect of the mutation and the activation barrier is again 20 kcal/mol, just as for wild-type EF-Tu with a neutral His84 (Table 1). However, the fact that the barriers for D21A are predicted to be very similar for the hydroxide mechanism with charged His84 (path i) and the fully concerted pathway (iii) with the neutral histidine would indicate that both alternatives may be accessible. This hypothesis actually seems to be supported by the finding that D21A shows a moderate pH dependence with a slope of 0.5,[11] which is what would be expected if the concerted mechanism with neutral His84 is partly responsible for the observed activity.

DISCUSSION

The results of our extensive free energy calculations on different possible GTP hydrolysis mechanisms of EF-Tu on the ribosome reveal a number of key features responsible for the overall catalytic effect. First, the most favorable reaction path (i) requires that His84 be doubly protonated and involves stabilization of negative charge development on the water nucleophile as a major part of the catalytic effect. Second, this effect is predominantly achieved both by the His84 side chain and by the backbone of the universally conserved PGH motif (for a comparison of the recent ribosome-bound EF-G structures, see also ref 42). In addition to these interactions, the effect of Asp21 is also to favor movement of one negative charge toward His84, while that of Lys24 is to eventually stabilize the final double negative charge on the β-phosphate. This situation is illustrated by the interaction energetics of key catalytic groups shown in Figure 5. There it can be seen that in the TS both His84 and the PGH backbone act to "pull" at the γ-phosphate negative charge, while Asp21 acts as to "push" it in the same direction. This is actually to some extent resisted by Lys24, which shows a destabilizing contribution in the TS (Figure 5). However, after inversion at the phosphorus atom has occurred and the second negative charge has migrated further

DOI: 10.1021/bi501373g
Biochemistry 2015, 54, 546−556

toward the β-phosphate, Lys24 exerts its stabilization of the product configuration.

The directionality of charge movement during the hydrolysis reaction is essentially built into the reaction center of the activated conformation both by the location of charged groups (Figure 1) and by the conformation of the backbone of the PGH motif. It is particularly noteworthy here that the catalytic conformation of the PGH backbone was predicted by our earlier simulations and has now been confirmed experimentally (Figure 2a). We suspect that other calculations on this system may suffer from using an incorrect conformation of the PGH backbone, which may explain why they obtained overly high activation barriers.[12,13] Unfortunately, it is somewhat difficult to make detailed comparisons with these works because they provide minimal structural information. Our results for the concerted neutral water attack (path iii) are, in fact, rather similar to those of ref 12, in which an activation barrier of 18 kcal/mol was obtained. However, in addition to the calculated barriers being too high, the fact that both our results (Table 1) and those of ref 12 show no effect of the H84Q mutation on this type of mechanism clearly speaks against it. In a subsequent study, Prasad et al.[40] suggested that the involvement of an extra water molecule in the reaction may further reduce the activation energy, and they also examined the hydroxide mechanism in which a barrier of 18 kcal/mol was predicted. However, those calculations were again based on the suboptimal EF-Tu structure, and in this respect, it should be emphasized that the PGH backbone conformation has the largest effect precisely on the hydroxide type of mechanism. This is because there is then significant negative charge development on the nucleophile. For neutral water attack, on the other hand, the PGH conformation is likely to be less important. Moreover, the crystal structures give no support to the notion that there is room for two water molecules between His84 and the γ-phosphate.[5,6]

With regard to the excellent recent experimental investigation of GTP hydrolysis by EF-Tu by Rodnina and co-workers,[11] a number of interesting connections can be made. First, in line with the observation that there is no significant kinetic solvent isotope effect on the ribosome reaction,[11] neither the present EVB simulations nor those of Warshel and co-workers[10,40] indicate that proton transfers are rate-limiting for the hydrolysis reaction. Second, our simulations show no catalytic advantage of a monovalent cation located between the α- and γ-phosphates. This is in agreement with the lack of GTP hydrolysis rate dependence on K^+ ion concentration found experimentally.[11] Instead, a plausible scenario is that such an ion is indeed present in the GTP complexes with the trGTPases before they are activated on the ribosome, and partly responsible for their intrinsic activity, but that this ion is then exchanged when the protonated His84 moves into its active conformation close to the γ-phosphate. Third, with regard to the different mutations studied, we find that the H84Q mutant is likely to cause a change in the reaction mechanism toward the neutral concerted water attack where it is predicted to yield a free energy barrier of 20 kcal/mol. This value is, in fact, in good agreement with the experimentally observed effect.[11] The same H84Q mutant is, however, predicted to make the hydroxide mechanism completely inaccessible as it destroys stabilization of charge development on the nucleophile.[10] Curiously, both ref 12 and ref 13 predicted the H84Q mutant to be faster than wild-type EF-Tu, which contradicts the experiments.

Finally, the D21A mutation seems to leave two different mechanistic options open. That is, with the hydroxide mechanism, a distinct destabilization of negative charge development on the nucleophile is predicted for the mutant. This is completely in line with the Asp21 effect discussed above, namely that it exerts a "push" of negative charge toward His84, and the loss of this push leads to a destabilization of the hydroxide ion state relative to the reactant state. The overall effect predicted for D21A on this type of mechanism is to increase the activation barrier to ~19 kcal/mol. However, the second option is that removal of the Asp21 negative charge could cause the His84 pK_a to decrease to a more normal value, thereby rendering the histidine side chain neutral. In that case, the free energy barrier predicted by our simulations becomes 20 kcal/mol, but now for the concerted neutral water attack mechanism. Both these values are in agreement with the experimentally observed effect, and it is therefore difficult to distinguish between them. However, the appearance of a significant pH dependence for the D21A mutant[11] may indicate that the latter type of mechanism is at least partly at play.

A general conclusion from our MD/EVB simulations of both wild-type and mutant versions of EF-Tu on the ribosome is that the GTP hydrolysis mechanism and rate are largely governed by the electrostatics of the reaction center. Here, the charges in the active site are perfectly balanced, as it were. Both ionized residues of EF-Tu and key Mg^{2+} ions observed in the crystal structures[5,6] make the reaction site overall neutral (Figure 1). Together with the strong dipole of the PGH backbone conformation,[5,6,10] the net effect is an electrostatic driving force for the reaction that leads to significant stabilization of the transition state. While it can be seen from these simulations that several different types of transition states are actually stabilized, to different extents, by the reaction center, it is clear from the calculations that negative charge development on the nucleophile is strongly favored. Hence, even though the hydroxide type of mechanism for GTP hydrolysis may not be viable in solution,[43] it is evident that the activated conformation of EF-Tu on the ribosome may favor such a reaction path.

■ ASSOCIATED CONTENT

Supporting Information

Different reaction schemes and their respective EVB parametrizations. This material is available free of charge via the Internet at http://pubs.acs.org.

■ AUTHOR INFORMATION

Corresponding Author

*E-mail: aqvist@xray.bmc.uu.se. Phone: +46 18 471 4109.

Funding

Support from the Swedish Research Council (VR), the Knut and Alice Wallenberg Foundation, and the Swedish National Infrastructure for Computing (SNIC) is gratefully acknowledged.

Notes

The authors declare no competing financial interest.

■ ACKNOWLEDGMENTS

We thank Mr. Christoffer Lind for conducting calculations of electron density maps.

■ ABBREVIATIONS

EF-Tu, elongation factor Tu; EF-G, elongation factor G; MD, molecular dynamics; FEP, free energy perturbation; EVB, empirical valence bond; PT, proton transfer.

DOI: 10.1021/bi501373g
Biochemistry 2015, 54, 546−556

REFERENCES

(1) Schmeing, T. M., and Ramakrishnan, V. (2009) What recent ribosome structures have revealed about the mechanism of translation. *Nature 461*, 1234−1242.

(2) Rodnina, M. V., and Wintermeyer, W. (2009) Recent mechanistic insights into eukaryotic ribosomes. *Curr. Opin. Cell Biol. 21*, 435−443.

(3) Daviter, T., Wieden, H. J., and Rodnina, M. V. (2003) Essential role of histidine 84 in elongation factor Tu for the chemical step of GTP hydrolysis on the ribosome. *J. Mol. Biol. 332*, 689−699.

(4) Vorhees, R. M., Schmeing, T. M., Kelley, A. C., and Ramakrishnan, V. (2010) The mechanism for activation of GTP hydrolysis on the ribosome. *Science 330*, 835.

(5) Tourigny, D. S., Fernandez, I. S., Kelley, A. C., and Ramakrishnan, V. (2013) Elongation factor G bound to the ribosome in an intermediate state of translocation. *Science 340*, 1235490.

(6) Chen, Y., Feng, S., Kumar, V., Ero, R., and Gao, Y. G. (2013) Structure of EF-G-ribosome complex in a pretranslocational state. *Nat. Struct. Mol. Biol. 20*, 1077−1084.

(7) Pulk, A., and Cate, J. H. D. (2013) Control of ribosomal subunit rotation by elongation factor G. *Science 340*, 1235970.

(8) Liljas, A., Ehrenberg, M., and Åqvist, J. (2011) Comment on "The mechanism for activation of GTP hydrolysis on the ribosome". *Science 333*, 37a.

(9) Vorhees, R. M., Schmeing, T. M., Kelley, A. C., and Ramakrishnan, V. (2011) Response to comment on "The mechanism for activation of GTP hydrolysis on the ribosome". *Science 333*, 37b.

(10) Wallin, G., Kamerlin, S. C. L., and Åqvist, J. (2013) Energetics of activation of GTP hydrolysis on the ribosome. *Nat. Commun. 4*, 1733.

(11) Maracci, C., Peske, F., Dannies, E., Pohl, C., and Rodnina, M. V. (2014) Ribosome-induced tuning of GTP hydrolysis by a translational GTPase. *Proc. Natl. Acad. Sci. U.S.A. 111*, 14418−14423.

(12) Adamczyk, A. J., and Warshel, A. (2011) Converting structural information into an allosteric energy-based picture for elongation factor Tu activation by the ribosome. *Proc. Natl. Acad. Sci. U.S.A. 108*, 9827−9832.

(13) Aleksandrov, A., and Fields, M. (2013) Mechanism of activation of elongation factor Tu by ribosome: Catalytic histidine activates GTP by protonation. *RNA 19*, 1−8.

(14) Kuhle, B., and Ficner, R. (2014) A monovalent cation acts a structural and catalytic cofactor in translational GTPases. *EMBO J.*, DOI: 10.15252/embj.201488517.

(15) Warshel, A. (1991) *Computer Modeling of Chemical Reactions in Enzymes and Solutions*, John Wiley & Sons, New York.

(16) Åqvist, J., and Warshel, A. (1993) Simulation of enzyme reactions using valence bond force fields and other hybrid quantum/classical approaches. *Chem. Rev. 93*, 2523−2544.

(17) Sund, J., Andér, M., and Åqvist, J. (2010) Principles of stop-codon reading on the ribosome. *Nature 465*, 947−950.

(18) Marelius, J., Kolmodin, K., Feierberg, I., and Åqvist, J. (1998) Q: A molecular dynamics program for free energy calculations and empirical valence bond simulations in biomolecular systems. *J. Mol. Graphics Modell. 16*, 213−225.

(19) Jorgensen, W. L., Maxwell, D. S., and Tirado-Rives, J. (1996) Development and testing of the OPLS all-atom force field on conformational energetics and properties of organic liquids. *J. Am. Chem. Soc. 118*, 11225−11236.

(20) King, G., and Warshel, A. (1989) A surface constrained all-atom solvent model for effective simulations of polar solutions. *J. Chem. Phys. 91*, 3647−3661.

(21) Parmeggiani, A., Kram, I. M., Okamura, S., Nielsen, R. C., Nyborg, J., and Nissen, P. (2006) Structural basis of the action of pulvomycin and GE2270 A on elongation factor Tu. *Biochemistry 45*, 6846−6857.

(22) Hilgenfeld, R., Mesters, J. R., and Hogg, T. (2000) Insights into the GTPase mechanism of EF-TU from structural studies. In *The Ribosome: Structure, Function, Antibiotics, and Cellular Interactions* (Garrett, R. A., et al., Eds.) ASM Press, Washington, DC.

(23) Trobro, S., and Åqvist, J. (2005) Mechanism of peptide bond synthesis on the ribosome. *Proc. Natl. Acad. Sci. U.S.A. 102*, 12395−12400.

(24) Ryckaert, J.-P., Ciccotti, G., and Berendsen, H. J. C. (1977) Numerical integration of cartesian equations of motion of a system with constraints: Molecular dynamics of n-alkanes. *J. Comput. Phys. 23*, 327−341.

(25) Lee, F. S., and Warshel, A. (1992) A local reaction field method for fast evaluation of long-range electrostatic interactions in molecular simulations. *J. Chem. Phys. 97*, 3100−3107.

(26) Bjelic, S., and Åqvist, J. (2006) Catalysis and linear free energy relationships in aspartic proteases. *Biochemistry 45*, 7709−7723.

(27) Eigen, M. (1964) Proton transfer, acid-base catalysis, and enzymatic hydrolysis. Part I: Elementary processes. *Angew. Chem., Int. Ed. 3*, 1−72.

(28) Åqvist, J. (1997) Modelling of proton transfer reactions in enzymes. In *Computational approaches to biochemical reactivity* (Náray-Szabó, G., and Warshel, A., Eds.) pp 341−362, Kluwer Academic Publishers, Dordrecht, The Netherlands.

(29) Kirby, A. J., and Younas, M. (1970) The reactivity of phosphate esters. Reactions of diesters with nucleophiles. *J. Chem. Soc. B 3*, 1165−1172.

(30) Kirby, A. J., Mederios, M., Oliveira, P. S. M., Orth, E. S., Brandao, T. A. S., Wanderlind, E. H., Amer, A., Williams, N. H., and Nome, F. (2011) Activating water: Important effects of non-leaving groups on the hydrolysis of phosphate triesters. *Chem.—Eur. J. 17*, 14996−15004.

(31) Åqvist, J., Kolmodin, K., Florian, J., and Warshel, A. (1999) Mechanistic alternatives phosphate monoester hydrolysis: What conclusions can be drawn from available experimental data? *Chem. Biol. 6*, R71−R80.

(32) Florian, J., and Warshel, A. (1997) A fundamental assumption about OH^- attack in phosphate ester hydrolysis is not fully justified. *J. Am. Chem. Soc. 119*, 5473−5474.

(33) Kirby, A. J., and Varvoglis, A. G. (1967) The reactivity of phosphate esters. Monoester hydrolysis. *J. Am. Chem. Soc. 89*, 415−423.

(34) Klähn, M., Rosta, E., and Warshel, A. (2006) On the mechanism of hydrolysis of phosphate monoester dianions in solutions and proteins. *J. Am. Chem. Soc. 128*, 15310−15323.

(35) Stockbridge, R. B., and Wolfenden, R. (2011) Enhancement of the rate of pyrophosphate hydrolysis by nonenzymatic catalysts and by inorganic pyrophosphatase. *J. Biol. Chem. 286*, 18538−18546.

(36) Afonine, P. V., Grosse-Kunstleve, R. W., and Adams, P. D. (2005) A robust bulk-solvent correction and anisotropic scaling procedure. *Acta Crystallogr. D61*, 850−855.

(37) Adams, P. D. (2010) PHENIX: A comprehensive Python-based system for macromolecular structure solution. *Acta Crystallogr. D66*, 213−221.

(38) Read, R. J. (1986) Improved Fourier coefficients for maps using phases from partial structures with errors. *Acta Crystallogr. D42*, 140−149.

(39) Jones, T. A., Zou, J. Y., Cowan, S. W., and Kjeldgaard, M. (1991) Improved methods for building protein in electron density maps and the location of errors in these models. *Acta Crystallogr. A47*, 110.

(40) Prasad, R. B., Plotnikov, N. V., Lameira, J., and Warshel, A. (2013) Quantitative exploration of the molecular origin of the activation of GTPase. *Proc. Natl. Acad. Sci. U.S.A. 110*, 20509−20514.

(41) Scheffzek, K., Ahmadian, M. R., Kabsch, W., Wiesmuller, L., Lautwein, A., Schmitz, F., and Wittinghofer, A. (1997) The Ras-RasGAP complex: Structural basis for GTPase activation and its loss in oncogenic Ras mutants. *Science 277*, 333−338.

(42) Yamamoto, H., Qin, Y., Achenback, J., Li, C., Kijek, J., Spahn, C. M. T., and Nierhaus, K. H. (2014) EF-G and EF4: Translocation and back-translocation on the bacterial ribosome. *Nat. Rev. Microbiol. 12*, 89−100.

(43) Lassila, J. K., Zalatan, J. G., and Herschlag, D. (2011) Biological phoshoryl transfer reactions: Mechanism and catalysis. *Annu. Rev. Biochem. 80*, 669−702.

DOI: 10.1021/bi501373g
Biochemistry 2015, 54, 546−556